Electrochemical Synthesis and Characterization of a New Electrochromic Copolymer Based on 2,2′-Bithiophene and Tris[4-(2-Thienyl)phenyl]amine

Shuang Chen[1,2], Qingxin Gao[2,1], Jinsheng Zhao[2,], Chuansheng Cui[2], Wei Yang[1], Xianxi Zhang[2,*]*

[1] College of Chemical Engineering, China University of Petroleum (East China), QingDao, 266580, P. R. China
[2] Shandong Key laboratory of Chemical Energy Storage and Novel Cell Technology, Liaocheng University, Liaocheng, 252059, P. R. China
[*]E-mail: j.s.zhao@163.com; zhangxianxi@lcu.edu.cn

A novel copolymer based on tris[4-(2-thienyl)phenyl]amine (TTPA) and 2,2′-bithiophene (BT) was electrochemically synthesized.Characterizations of the resulting copolymer P(TTPA-co-BT) were performed by cyclic voltammetry (CV), UV–vis spectroscopy, Fourier transform infrared spectroscopy(FT-IR), scanning electron microscopy (SEM). The P(TTPA-co-BT) film had distinct electrochromic properties from both the PTTPA and the PBT homopolymers, and exhibited three different colors (claybank, grass green, and blue) under various potentials. Moreover, the copolymer film showed high optical contrasts (48.46% at 435 nm and 33.46% at 820 nm) and satisfactory response times (1.92 s at 435 nm and 1.83 s at 820 nm). An electrochromic device (ECD) based on P(TTPA-co-BT) and poly(3,4-ethylenedioxythiophene) (PEDOT) was constructed and characterized. The ECD was found to have a high optical contrast, fast response time, satisfactory optical memories and good redox stability.

1. INTRODUCTION

Over the past decade, lots of attentions have been focused on the class of conjugated polymers owing to their unique electronic and optical properties [1]. Recent advances of conducting polymers (CPs) have been widely applied in many fields such as electrochromic devices [2,3], polymer solar cells [4], sensors [5], light emitting diodes [6], membranes [7]. For CPs, electrochromism is defined as the property inherent in some materials which enable them to electrochemically switch between

different colored states as a result of oxidation–reduction reaction [8]. It results from the generation of different electronic absorption bands that correspond to changes between at least two states [9]. Electronic absorption shifts bathochromically upon oxidation process, and the color contrast between redox states is related to the polymer band gap [10].

Copolymerization is an easy, facile method to control the electrochromic properties of conducting polymers. This procedure allows one to obtain materials with controlled properties without suffering the experimental disadvantages associated to the preparation of new homopolymers, i.e. complex synthetic routes to develop sophisticated monomers [11]. Thus, copolymerization of distinct monomers or homopolymerization of hybrid monomers containing several distinct units can lead to interesting combination of the properties observed in the corresponding homopolymers [12].

As one of the useful hole transporting materials, triphenylamine (TPA) and its organic and polymeric derivatives have been widely used in organic and polymeric optoelectronic devices with optical and charge-transport properties [13]. Liou *et al*. have reported the synthesis and properties of several TPA-containing polyimides which showed interesting electrochromic properties such as multichromism, good reversibility and mechanical stability [14,15]. In addition, thiophene-containing triarylamine polymers have been drawn increasing attention because of their high stability to electrochemical oxidation and redox switching and even their optoelectronic properties [16].
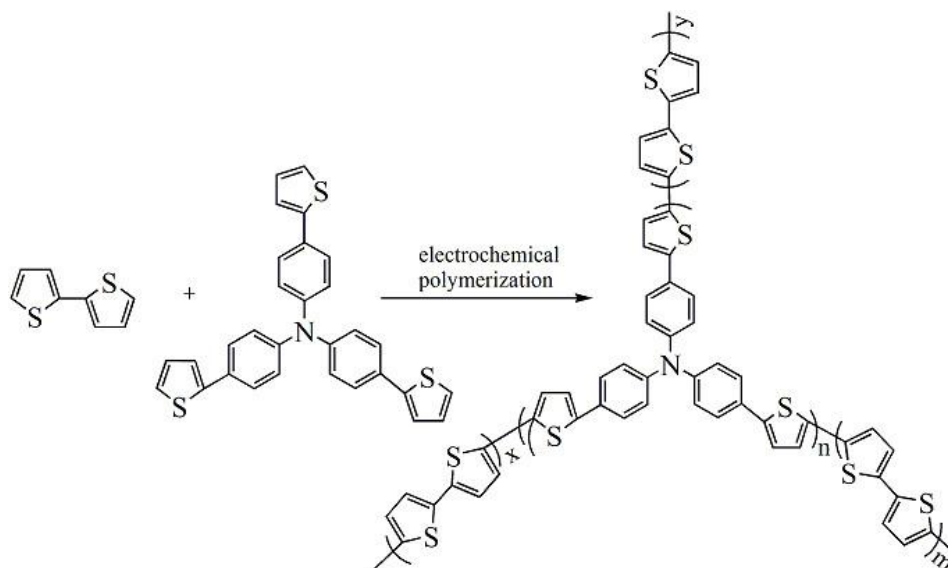
Scheme 1. Synthetic route of the copolymer of BT and TTPA.

Recently, we also made a study on the electrochromic properties of the elelctrochemically synthesized poly(tris[4-(2-thienyl)phenyl]amine) (PTTPA) and its application in electrochromic device, which showed the perspective of thiophene-containing triarylamine polymers as multichromic materials [17]. On the other hand, much of our recent interests has been focused on the copolymerization in order to prepare conducting polymers with specifically desired properties. Poly(2,2′-bithiophene) (BT) presents the properties of rapid switching and excellent stability in its

doped form. And, BT has been shown a ideal monomer candidate besides 3,4-Ethylenedioxythiophene (EDOT) for copolymer synthesis due to the fact that some copolyers based on BT exhibitted multichromism or a tunable electrochromism [18,19].

According to above considerations, copolymers based on TTPA and BT were successfully synthesized via the electrochemical oxidation of BT/TTPA mixtures in ACN/DCM (1:1, by volume) solution containing 0.2 M NaClO$_4$ as a supporting electrolyte (Scheme 1). The electrochromic and spectroelectrochemical properties of the copolymer were studied in detail. The copolymer film revealed three different colors (claybank, grass green, and blue). To explore the use of this material in electrochromic device we constructed a dual-type electrochromic device with ITO/copolymer/gel electrolyte/PEDOT/ITO configuration, where the copolymer and PEDOT functioned as the anodically and the cathodically coloring layers respectively. Characterizations of the electrochromic behavior of the copolymer and the device were achieved by spectroelectrochemistry, kinetic, colorimetry studies.

2. EXPERIMENTAL

2.1. Materials

The tris[4-(2-thienyl)phenyl]amine monomer was synthesized as reported previously by our group [17]. 2,2′-Bithiophene (BT) and 3,4-ethylenedioxythiophene (EDOT, 98%) were purchased from Aldrich Chemical. Dichloromethane(DCM, Shanghai Chemical Reagent Company), Commercial high-performance liquid chromatography grade acetonitrile (ACN, Tedia Company, INC., USA), poly(methyl methacrylate) (PMMA, Shanghai Chemical Reagent Company), propylene carbonate (PC, Shanghai Chemical Reagent Company) and lithium perchlorate (LiClO$_4$, Shanghai Chemical Reagent Company, 99.9%) were used directly without further purification. Sodium perchlorate (NaClO$_4$, Shanghai Chemical Reagent Company, 98%) was dried in vacuum at 60 ºC for 24 h before use. Other reagents were all used as received without further treatment. Indium-tin-oxide-coated (ITO) glass (Sheet resistance: < 10 Ω $\square^{-1}$, purchased from Shenzhen CSG Display Technologies, China) was washed with ethanol, acetone and deionized water successively under ultrasonic, and then dried by N$_2$ flow.

2.2. Instrumentation

^{1}H NMR spectroscopy studies were carried out on a Varian AMX 400 spectrometer and tetramethylsilane (TMS) was used as the internal standard for ^{1}H NMR. FT-IR spectra were recorded on a Nicolet 5700 FT-IR spectrometer, where the samples were dispersed in KBr pellets. Scanning electron microscopy (SEM) measurements were taken by using a Hitachi SU-70 thermionic field emission SEM. UV–vis spectra were carried out on a Perkin-Elmer Lambda 900 UV–vis–near-infrared spectrophotometer. Digital photographs of the polymer films and device cell were taken by a Canon Power Shot A3000 IS digital camera.

2.3. Electrochemistry

Electrochemical syntheses and experiments were performed in a one-compartment cell with a CHI 760 C Electrochemical Analyzer (Shanghai ChenHua Instrument Co. China) under control of a computer. The working electrodes was a platinum wires with a diameter of 0.5 mm, a platinum ring worked as counter electrode, and a silver wire (Ag wire) was taken as pseudo reference electrode. The working and counter electrodes for cyclic voltammetric experiments were placed 0.5 cm apart during the experiments. All electrochemical polymerization and CV tests were taken in ACN/DCM (1:1, by volume) solution containing 0.2 M $NaClO_4$ as a supporting electrolyte. The pseudo reference electrode was calibrated externally using a 5 mM solution of ferrocene (Fc/Fc$^+$) in the electrolyte ($E_{1/2}$(Fc/Fc$^+$) = 0.25 V vs. Ag wire in ACN/DCM (1:1, by volume) solution containing 0.2 M $NaClO_4$). All the potentials mentioned follow were vs. the Ag wire electrode [16]. The half-wave potential ($E_{1/2}$) of Fc/Fc$^+$ measured in ACN/DCM (1:1, by volume) solution containing 0.2 M $NaClO_4$ was 0.28 V vs. SCE. Thus, the potential of Ag wire was assumed to be 0.03 V vs. SCE. All of the electrochemical experiments were carried out at room temperature under nitrogen atmosphere. The amount of polymers deposited on platinum electrode was controlled by the integrated charge passed through the cell for electrochemical tests. Cyclic voltammetry(CV) of polymer was carried out with the same electrode set-up in monomer-free electrolyte solution.

2.4. Preparation for measurements

To obtain sufficient amount of polymers for spectra analysis and SEM measurements, a three-electrode cell assembly was used where the working electrode was an ITO glass with a surface area of 0.9×2.0 cm^2, the counter electrode was a stainless steel wire, and an Ag wire was used as pseudo-reference electrode.The copolymer films for spectroelectrochemistry were prepared by potentiostatically deposition on ITO electrode. After electrochemical polymerization, electrochemical dedoping was carried out in ACN/DCM (1:1, by volume) containing 0.2 M $NaClO_4$ for 30 minites. Then the copolymer was washed with ACN/DCM (1:1, by volume) for 3 times to remove the supporting electrolyte and oligomers/monomers.

2.5. Characterizations

The obtained copolymer films were studied by cyclic voltammetry and spectroelectrochemistry. Spectroelectrochemical data were recorded on Perkin-Elmer Lambda 900 UV–vis–near-infrared spectrophotometer connected to a computer. Scanning electron microscopy (SEM) measurements were taken by using a using JEOL JSM-6380LV SEM (JEOL Ltd., Tokyo, Japan). Digital photographs of the polymer films were taken by a Canon Power Shot A3000 IS digital camera.

2.6. Preparation of the gel electrolyte

A gel electrolyte based on PMMA and LiClO$_4$ was plasticized with PC to form a highly transparent and conductive gel. ACN was also included as a high vapor pressure solvent to allow an easy mixing of the gel components. The composition of the casting solution by weight ratio of ACN:PC:PMMA:LiClO$_4$ was 70:20:7:3. The gel electrolyte was used for construction of the polymer cell [17].

2.7. Construction of electrochromic devices

Electrochromic devices (ECDs) were constructed using two complementary polymers, namely P(TTPA-co-BT) as the anodic material and PEDOT as the cathodic material. Both P(TTPA-co-BT) and PEDOT films were electrodeposited on two ITO glass (the active area: 1.8 cm × 2.0 cm) at +1.4 V. Electrochromic device was built by arranging the two polymer films (one oxidized, the other reduced) facing each other separated by a gel electrolyte.

3. RESULTS AND DISCUSSION

3.1 Electrochemical polymerization and characterizations

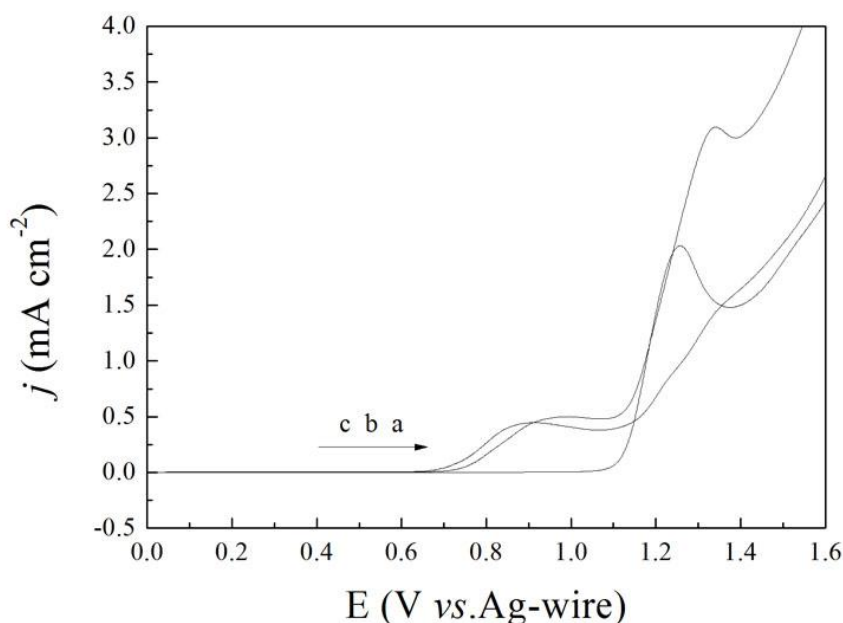#### 3.1.1. Electrochemical polymerization

Figure 1. Anodic polarization curves of (a) 0.004 M BT, (b) 0.004 M BT and 0.004 M TTPA, (c) 0.004 M TTPA in ACN/DCM containing 0.2 M NaClO$_4$ at a scan rates of 100 mV s^{-1}. *j* denotes the current density, E denotes the potential.

The anodic polarization curves of 0.004 M BT and 0.004 M TTPA in ACN/DCM (1:1, by volume) solution containing 0.2 M $NaClO_4$ are shown in Fig. 1. The onset oxidation potential (E_{onset}) of BT and TTPA in the solution are approximately +1.11 V (Fig. 1a) and +0.71 V (Fig. 1c), respectively. It is well known that successful electrochemical copolymerization of different monomers is due to the fact that the E_{onset} of the monomers are close to each other [18, 19]. However the distinction of the E_{onset} between BT and TTPA is 0.4 V. As can been seen from Fig. 1b, the E_{onset} of the BT/TTPA at 1:1 mixture is +0.74 V, which is intervenient between BT and TTPA, indicating the existence of the interaction between two monomers in ACN/DCM (1:1, by volume) solution containing 0.2 M $NaClO_4$ [20, 21]. The synthetic route of the copolymer of TTPA and BT is illustrated in Scheme 1.

Fig. 2 displays the successive cyclic voltammogram (CV) curves of 0.004 M BT, 0.004 M TTPA and the BT/TTPA mixture at 1:1 (0.004 M BT and 0.004M TTPA) in ACN/DCM solution containing 0.2 M $NaClO_4$ at a potential scan rate of 100 mV s^{-1}. As the CV scan continued, polymer films are formed on the working electrode surface. The increase in the redox wave current densities implies that the amount of conducting polymers deposited on the electrode is increasing[20].
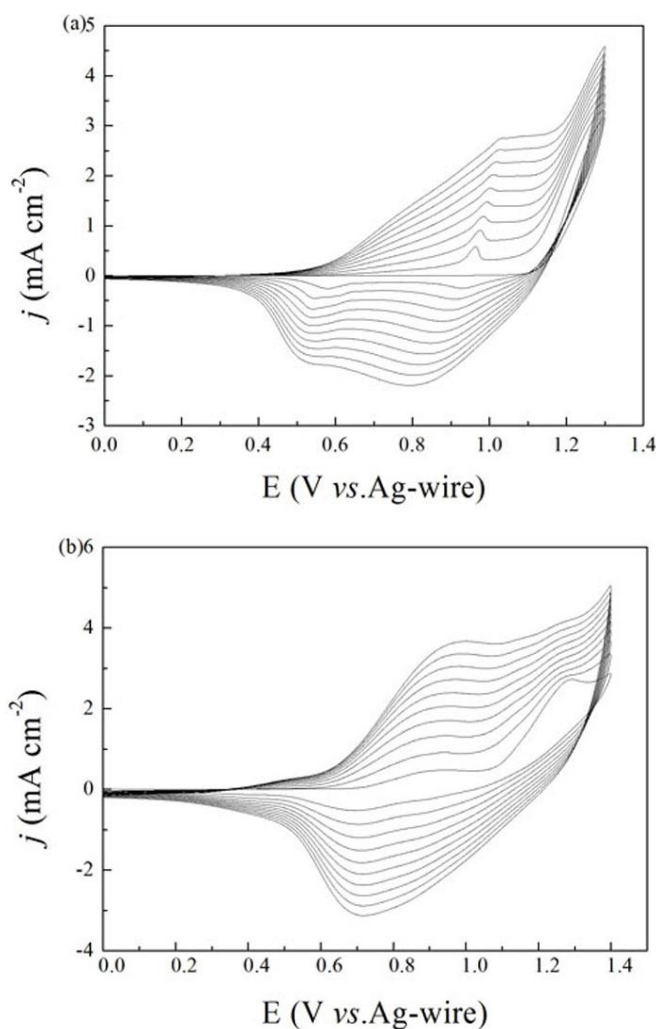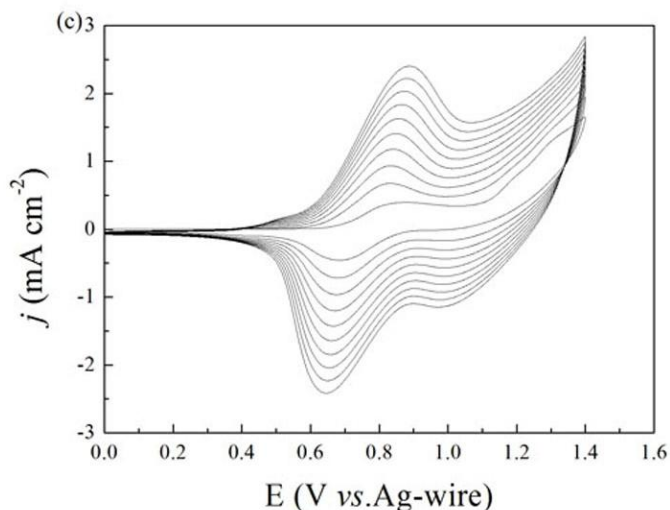
Figure 2. Successive CV curves of (a) 0.004 M BT, (b) the mixture of 0.004 M BTand 0.004 M TTPA, (c) 0.004 M TTPA in ACN/DCM containing 0.2 M NaClO$_4$. Scanning rates: 100 mV s^{-1}. *j* denotes the current density, E denotes the potential.

In Fig. 2a, the CV curves of BT show a sharp oxidation peak at 1.03 V and two successive reduction peaks at 0.55 and 0.83 V, respectively.

The CV curves of TTPA (Fig. 2c) show an anodic peak at 0.88 V, and two cathodic peaks at 0.64 and 0.97 V, respectively. However, the CV curve of the BT/TTPA mixture at 1:1 exhibits an anodic peak and a cathodic peak at +0.98V and +0.71 V, respectively (Fig. 2b), which is different from those of BT and TTPA, indicating the formation of a new polymer consisting of both BT and TTPA units [22-24]. These can show evidence of copolymer formation, and yet to be supported by other characterization techniques.
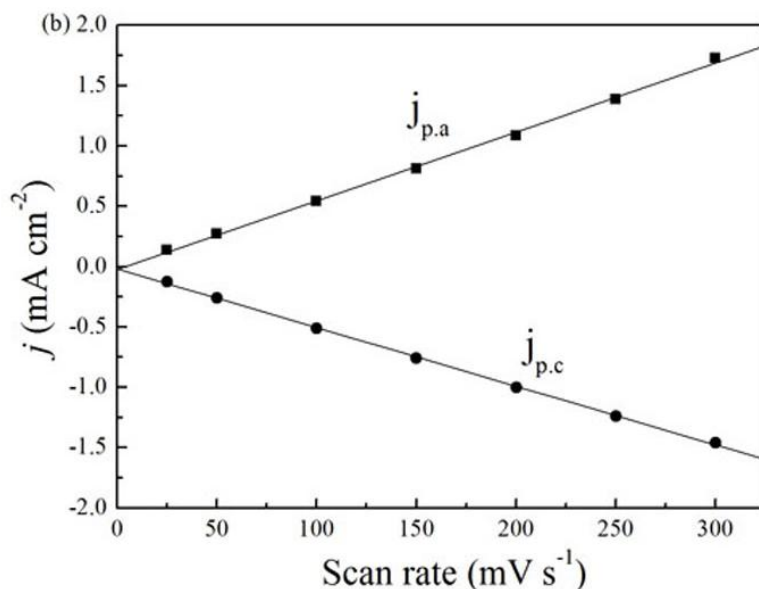
3.1.2. Electrochemistry of the P(BT-co-TTPA) film
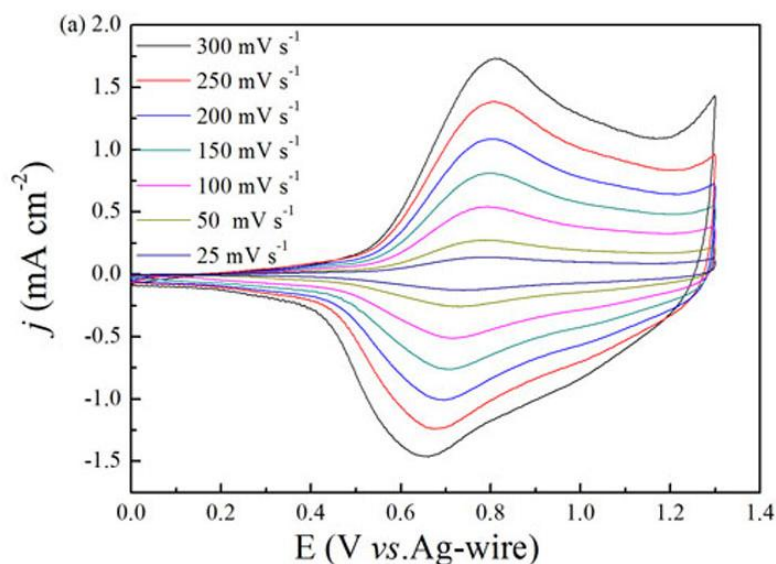
Figure 3. (a) CV curves of the copolymer at different scan rates in the monomer-free solution of ACN/DCM containing 0.2 M NaClO$_4$. (b) scan rate dependence of the anodic and cathodic peak current densities graph. $j_{p.a}$ and $j_{p.c}$ denote the anodic and cathodic peak current densities, respectively.

Fig. 3(a) shows the CV curves of the P(TTPA-co-BT) film (prepared with the feed ratio of BT/TTPA at 1:1 on platinum wire by sweeping the potentials from 0 V and +1.4 V) at different scanning rates between 25 and 300 mV s^{-1} in a monomer-free solution of ACN/DCM (1:1, by volume) containing 0.2 M NaClO$_4$. The copolymer film exhibited a reversible redox process at 0.64~0.80 V. The peak current densities (j) are proportional to the potential scan rates (Fig. 3(b)), indicating that the copolymer film is electroactive and adheres well to the electrode [25]. In addition, anodic and cathodic peak currents reveal a linear relationship as a function of scan rate for the copolymer, implying that the electrochemical processes of the copolymer are reversible and not diffusion limited [26].

3.1.3. Morphology

Scanning electron micrographs (SEM) of polymers provide their clear surface and bulk morphologies, which are closely related to their optical and electrical properties [27]. Fig. 4 gives the SEM images of PBT, P(TTPA-co-BT) and PTTPA, which were prepared on ITO electrodes potentiostatically and dedoped before characterization. As shown in Fig. 4a, PBT exhibits a coral structure with smaller grains. PTTPA film reveals clusters of small particles (Fig. 4c). However, the copolymer exhibites a intermediate state between PBT and PTTPA (Fig. 4b). The difference of morphology between copolymer and homopolymers also confirms the occurrence of copolymerization between BT and TTPA units.
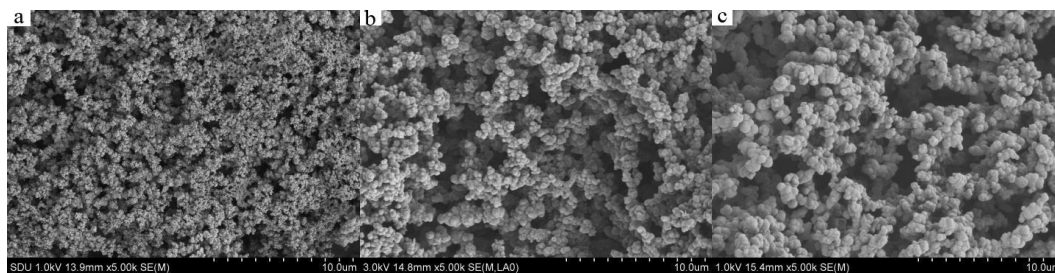
Figure 4. SEM images of (a) BT, (b) P(BT-co-TTPA) and (c) PTTPA deposited potentiostatically on ITO electrode.

3.1.4. UV–vis spectra of polymers

Fig. 5 depicts the UV–vis spectra of dedoped PBT, PTTPA and copolymers based on BT and TTPA deposited on ITO electrode with the same polymerization charge (3.2×10^{-2} C). For PBT film (Fig. 5a), there is a wide and strong absorption peak at 446 nm. On the other hand, the spectrum of PTTPA film shows a broad absorption at 428 nm (Fig. 5e). While, the maximum absorption peaks of the obtained copolymers with 3:2, 1:1 and 2:3 BT/TTPA feed ratios are at 440, 437 and 434 nm, respectively. However, there is a little bit blue shift of the main absorption of copolymer film in contrast to pure PBT due to the incorporation unit of TTPA, further confirming the occurrence of copolymerization [23]. Fine tuning in the band gap is achieved by tailoring the co-monomer feed ratio of copolymerization. Furthermore, the colors of polymers films on ITO at dedoped and doped states were also recorded, as shown in the insets of Fig. 5. PBT displays a reddish brown color in dedoped state and a gray color in doped state (see insets A and A′), and PTTPA switchs from grassy yellow to bluish green (see insets C and C′). While, P(BT-co-TTPA) changes color from claybank (inset B) to bule (inset B′). The colors of P(BT-co-TTPA) are significantly different from those of two individual homopolymers, further confirming the formation of copolymer consisting of both BT and TTPA units.

Besides, the optical band gap (E_g) of polymer is deduced from the absorption band edges (λ_{onset}). copolymers with 3:2, 1:1 and 2:3 BT/TTPA feed ratios are at 440, 437 and 434 nm, respectively.The E_g of copolymers with 3:2, 1:1 and 2:3 BT/TTPA feed ratios were calculated as 2.13 eV, 2.16 eV and 2.28 eV, respectively, which was lower than that of PBT (1.98 eV) and higher than that of PTTPA (2.45 eV). The effect of copolymerization between BT and TTPA leads to an obvious increase in the E_g comparing with that of PBT, which implies that the introduction of TTPA units into PBT can tune the conjugation of the copolymer.

Table 1 summarizes the onset oxidation potential (E_{onset}), maximum absorption wavelength (λ_{max}), low energy absorption edges (λ_{onset}), HOMO and LUMO energy levels and the optical band gaps (E_g) values of PBT, PTTPA and the copolymers (prepared with the feed ratio of BT/TTPA at 3:2 (COP1), 1:1 (COP2) and 2:3 (COP3), respectively) quite clearly. HOMO energy levels of them are calculated by using the formula $E_{HOMO} = -e(E_{onset} + 4.43)$ (vs. SCE) and LUMO energy levels (E_{LUMO}) of them are calculated by the subtraction of the optical band gap (E_g) from the HOMO levels [28].
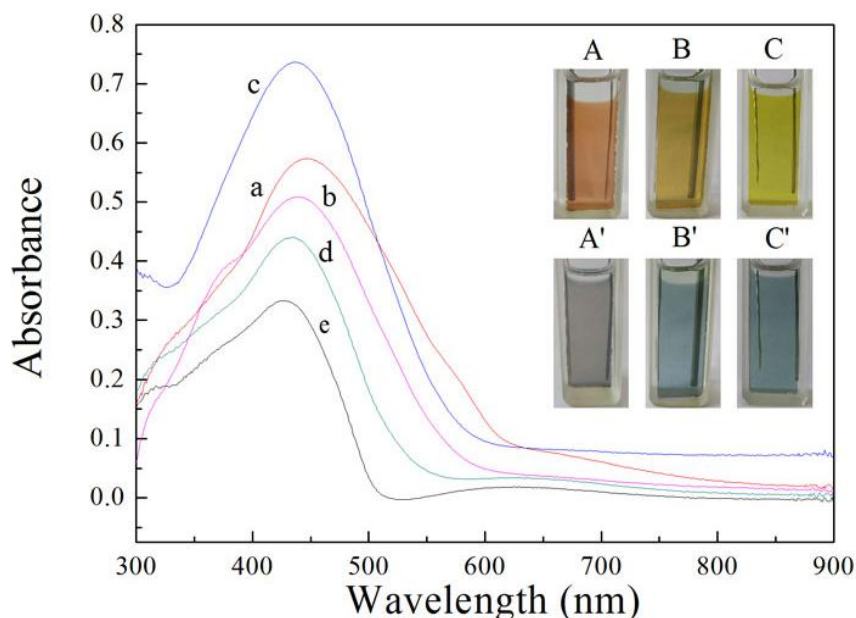
Figure 5. UV–vis spectra of dedoped (a) BT, the copolymers prepared with the feed ratio of BT/TTPA at (b) 3:2 (COP1), (c) 1:1 (COP2) and (d) 2:3 (COP3), respectively, and (e) PTTPA deposited on ITO at the neutral state. Insets: (A) reddish brown, (B) claybank, (C) glassy yellow are dedoped films, and (A′) gray, (B′) bule, (C′) bluish green are doped films of PBT, P(BT-co-TTPA) and PTTPA, respectively.

Table 1. The onset oxidation potential (E_{onset}), maximum absorption wavelength (λ_{max}), low energy absorption edges (λ_{onset}), HOMO and LUMO energy levels and optical band gap (E_g) values of PBT, PTTPA, and the copolymers (prepared with the feed ratio of BT/TTPA at 3:2, 1:1 and 2:3, respectively).

Compounds	E_{onset},vs.(Ag-wire) (V)	λ_{max} (nm)/ λonset (nm)	$E_g{}^a$ (eV)	HOMO (eV)	LUMO[b] (eV)
PBT	0.64	446/627	1.98	-5.07	-3.09
COP1	0.59	440/583	2.13	-5.02	-2.89
COP2	0.56	437/575	2.16	-4.99	-2.83
COP3	0.52	434/544	2.28	-4.95	-2.67
PTTPA	0.50	428/507	2.45	-4.93	-2.48

[a] Calculated from the low energy absorption edges (λ_{onset}).

[b] Calculated by the subtraction of the optical band gap (E_g) from the HOMO level.

3.2. Electrochromic properties of P(BT-co-TTPA) film

3.2.1 Spectroelectrochemical properties of P(BT-co-TTPA) film

Spectroelectrochemistry is a useful method for studying the changes in the absorption spectra and the information about the electronic structures of conjugated polymers as a function of the applied voltage [29]. The P(TTPA-co-BT) film coated ITO was switched between neutral (+0 V) and doped

(+1.3 V) states in ACN/DCM solution containing 0.2 M NaClO$_4$ in order to obtain the in situ UV–vis spectra (Fig. 6). At the neutral state, the copolymer film exhibits a absorption band at 435 nm due to the π-π* transition. The intensity of the P(TTPA-co-BT) π–π* electron transition absorption decreases while a charge carrier absorption band located at around 650 nm increase dramatically upon oxidation. The appearance of charge carrier bands can be attributed to the evolution of polaron and bipolaron bands [30].
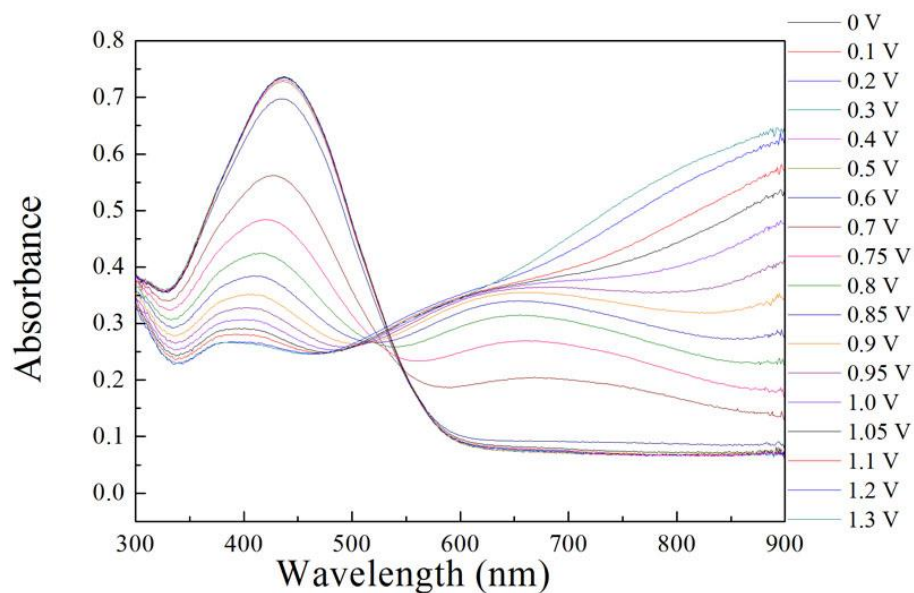

Figure 6. Spectroelectrochemical spectra of P(BT-co-TTPA) with applied potentials between 0V and +1.3 V in monomer-free ACN/DCM solution containing 0.2 M NaClO$_4$.

Figure 7. Colors of the P(TTPA-co-BT) film at different applied potentials in ACN /DCM solution containing 0.2 M NaClO$_4$.

In addition, it was interesting to find that the P(TTPA-co-BT) film showed a multicolor electrochromism. In order to study the range of colors, a wide interval of potentials (0 V to +1.4 V) is

applied on the as-prepared P(TTPA-co-BT) films. As can be seen from Fig. 7, P(TTPA-co-BT) film shows three different colors in neutral and oxidized states. The claybank color of the film at neutral state (0 V) turns into grass green (+0.8 V) at intermedia doped state, and then into blue color at full doped state (+1.4 V). This multicolor property possesses significant potential applications in smart windows or displays and so on [31].

3.2.2 Electrochromic switching of P(TTPA-co-BT) film in solution

It is important that polymers can switch rapidly and exhibit a noteworthy color change for electrochromic applications [32]. For this purpose, double potential step chronoamperometry technique was used to investigate the switching ability of P(TTPA-co-BT) film between its neutral and full doped state (Fig. 8) [33]. The dynamic electrochromic experiment for P(TTPA-co-BT) film was carried out at 435 and 820 nm, respectively. The potential was interchanged between 0 V (the neutral state) and +1.4 V (the oxidized state) at regular intervals of 4 s. One important characteristic of electrochromic materials is the optical contrast ($\Delta T\%$), which can be defined as the transmittance difference between the redox states. The $\Delta T\%$ of the P(BT-co-TTPA) was calculated to be 33.46 % at 435 nm and 48.46 % at 820 nm, as shown in Fig. 8.

The coloration efficiency (CE) is also an important characteristic for the electrochromic materials. CE can be calculated by using the equations and given below [34]:

$$\Delta OD = \log\left(\frac{T_b}{T_c}\right) \text{ and } \eta = \frac{\Delta OD}{\Delta Q}$$

where T_b and T_c are the transmittances before and after coloration, respectively. ΔOD is the change of the optical density, which is proportional to the amount of created color centers. η denotes the coloration efficiency (CE). ΔQ is the amount of injected charge per unit sample area. CE of P(TTPA-co-BT) film was measured as 114.4 cm^2 C^{-1} (435 nm) and 136.9 cm^2 C^{-1} (820 nm), respectively, which had reasonable coloration efficiency.

Response time, one of the most important characteristics of electrochromic materials, is the time needed to perform a switching between the neutral state and oxidized state of the materials [26]. As shown in Fig. 8b, the response required to attain 95% of total transmittance difference was found to be 1.92 s from the reduced to the oxidized state and 1.18 s from the oxidized to the reduced state at 435 nm, 1.83 s from the reduced to the oxidized state and 0.89 s from the oxidized to the reduced state at 820 nm. Thus, P(TTPA-co-BT) can be rapidly switched to the reduced state, which can be attributed to the ease of charge transport in the conducting film when it is reduced [35]. Based on the discussion, the distinct optical contrast, the satisfactory coloration efficiency and switching property make this P(TTPA-co-BT) a promising electrochromic material.
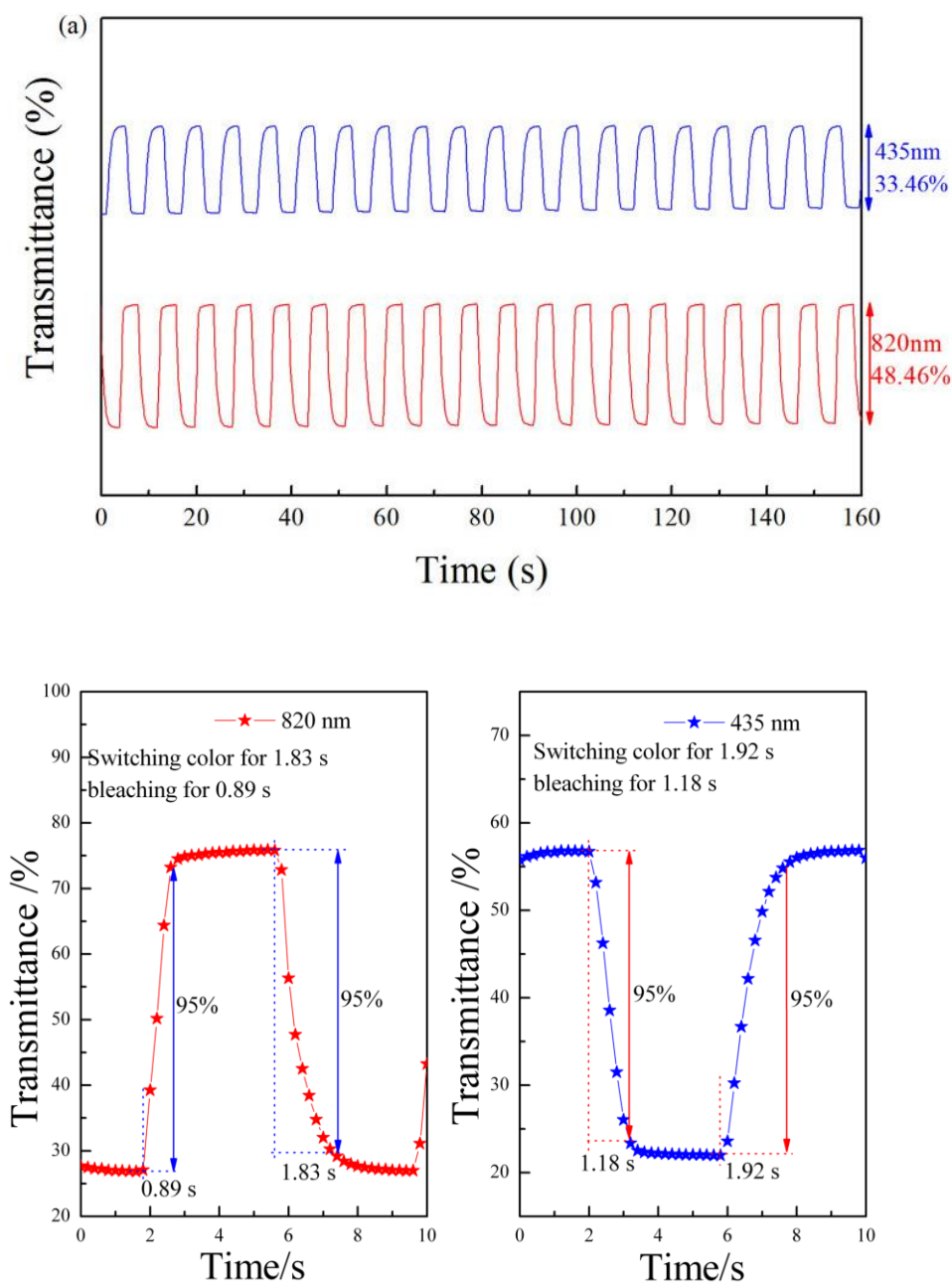
Figure 8. (a) Electrochromic switching for P(TTPA-co-BT) film under an applied square voltage signal between 0 V and +1.40 V with a residence time of 4 s at 435 nm and 820 nm, respectively.(b) One cycle of P(TTPA-co-BT) film's electrochromic switching.

3.3. Spectroelectrochemistry of electrochromic devices（ECDs）

3.3.1 Spectroelectrochemical properties of ECD

A dual type ECD consisting of P(TTPA-co-BT) and PEDOT constructed and its spectroelectrochemical behaviors were also studied. Before composing the ECD, the anodic polymer film (P(TTPA-co-BT)) was fully reduced and the cathodic polymer film (PEDOT) was fully oxidized. The P(TTPA-co-BT)/PEDOT device was switched between –0.8 and +1.6 V. The

spectroelectrochemical results are shown in Fig. 9. At –0.8 V, the P(TTPA-co-BT) layer was in its neutral state and PEDOT was in oxidized state and the device color was grayish green. Thus, there was maximum absorption at around 443 nm due to π-π* transition of the electrochromic layer of P(TTPA-co-BT). As the applied potential increased, the P(TTPA-co-BT) layer started to be oxidized and the intensity of the peak due to the π-π* transition decreased, while PEDOT layer was reduced and evolution of a new intense absorption at around 640 nm (π-π* transition of PEDOT itself), and the dominated color of the device was blue at +1.4 V.
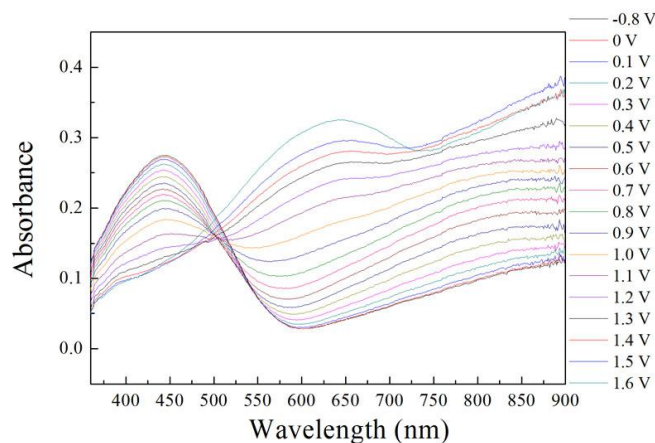

Figure 9. Spectroelectrochemical spectra of the P(TTPA-co-BT)/PEDOT device at various applied potentials between −0.8 and +1.6 V.

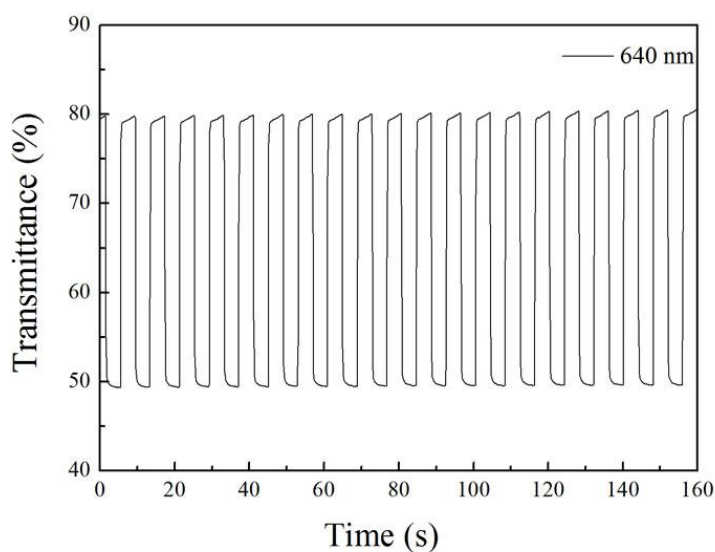### 3.3.2. Switching of ECD

Figure 10. Electrochromic switching, optical transmittance change monitored at 630 nm for P(TTPA-co-BT)/PEDOT device between 0 V and +1.4 V with a residence time of 4 s.

Kinetic studies were also done to test the percent transmittance changes and the response time of P(TTPA-co-BT)/PEDOT ECD. Under a potential input of 0 and +1.4 V at regular intervals of 4 s, the optical response at 640 nm, as illustrated in Fig. 10. The response time is found to be 0.38 s at 95% of the maximum transmittance difference from the neutral state to oxidized state and 0.33 s from the oxidized state to the neutral state, and optical contrast ($\Delta T\%$) is calculated to be 30.58%.

3.3.3 Open circuit memory of ECD

The optical memory in the electrochromic devices is an important parameter because it is directly related to its application and energy consumption during the use of ECDs [37]. The optical spectrum for P(TTPA-co-BT)/PEDOT device was monitored at 640 nm as a function of time at 0 V and +1.4 V by applying the potential for 1 s for each 100 s time interval. As shown in Fig. 11, at light yellow colored state device showed a true permanent memory effect since there was almost no transmittance change under applied potential or open circuit conditions. In blue colored state device was rather less stable in terms of color persistence, however this matter can be overcome by application of current pulses to freshen the fully colored states.
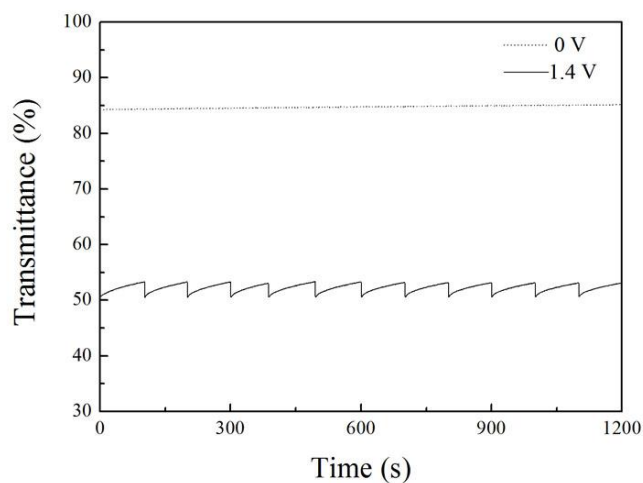

Figure 11. Open circuit stability of the P(CPDT-co-NMPy)/PEDOT device monitored at 630 nm.

3.3.4 Stability of the ECD

The stability of the devices toward multiple redox switching usually limits the utility of electrochromic materials in ECD applications. Therefore, redox stability is another important parameter for ECD [38]. For this reason, the P(TTPA-co-BT)/PEDOT device was tested by cyclic voltammetry of the applied potential between −0.8 V and +1.6 V with 500 mV s^{-1} to evaluate the stability of the device (Fig. 12). After 500 cycles, 93.98% of its electroactivity is retained and there is no obvious decrease of activity between 500 cycles and 1000 cycles. These results show that this device has good redox stability.
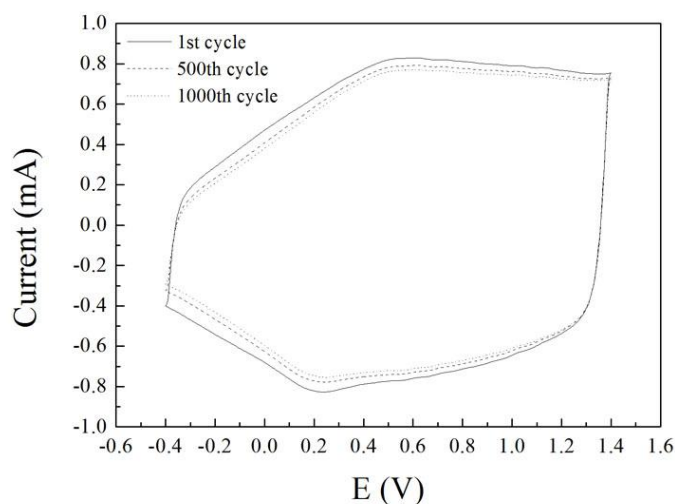
Figure 12. Cyclic voltammogram of P(TTPA-co-BT)/PEDOT device as a function of repeated with a scan rate of 500 mV/s.

4. CONCLUSION

A new copolymer based on TTPA and BT was successfully synthesized by electrochemical oxidation of the monomers mixture in ACN/DCM (1:1, by volume) solution containing 0.2 M $NaClO_4$. Cyclic voltammetry, UV–vis, FT-IR analyses and scanning electron microscopy confirmed that the resulting polymer was a copolymer rather than a blend or a composite of the respective homopolymers. Furthermore, the P(TTPA-co-BT) film had distinct electrochromic properties and exhibited three different colors (claybank, grass green and blue) under various potentials. The copolymer film showed high optical contrasts (48.46% at 435 nm and 33.46% at 820 nm) and satisfactory response times (1.92 s at 435 nm and 1.83 s at 820 nm). The dual type electrochromic device (ECD) based on P(TTPA-co-BT) and PEDOT was constructed and its electrochromic properties were also studied. Also electrochromic device based on P(TTPA-co-BT) and PEDOT was constructed and characterized. Electrochromic switching study revealed that copolymerization with TTPA can enhance the electrochromic properties. For the device, maximum contrast and response time were 30.83% and 0.33 s at 640 nm. This ECD also shows satisfactory optical memories and redox stability. Considering these features, this device is a promising candidate for commercial applications.

References

1. D.J. Liaw, K.L. Wang, S.P. Pujari, Y.C. Huang, B.C. Tao, M.H. Chen , K.R. Lee and J.Y. Lai, *Dyes and Pigments* . 82 (2009) 109–117.
2. G.M. Nie, L.J. Zhou, Q.F. Guo, S.S Zhang, *Electrochem. Commun*. 12 (2010)160-163.
3. J.H. Kang, Z.C. Xu, S.M. Paek, F. Wang, S.J. Hwang, J. Yoon, J.H. Choy, *Chem. Asian J*. 6 (2011) 2123–2129.
4. S. Gunes, H. Neugebauer and N. S. Sariciftci, *Chem. Rev*. 107 (2007) 1324–1338.
5. H. Zhang, J. Zhao, H. Liu, H. Wang, R. Liu, J. Liu, *Int. J. Electrochem. Sci*. 5 (2010) 295-301.
6. A. Kraft, A.C. Grimsdale, A.B. Holmes, *Angew. Chem. Int. Ed*. 37 (1998) 402.
7. C.R. Martin, W. Liang, V. Menon, R. Parthasarathy, A. Parthasarathy, *Synth. Met*. 57 (1993) 3766–3773.
8. H. Seol, H. Jeong, S. Jeon, *J. Electroanal. Chem*. 636 (2009) 107–112.
9. W.R. Lian, K.L. Wang, J.C. Jiang, D.J. Liaw, K.R. Lee, J.Y. Lai, *J. Polym. Sci.: Part A: Polym. Chem.* 49 (2011) 3248–3259.
10. B. Yigitsoy, S. Varis, C. Tanyeli, I.M. Akhmedov, L. Toppare, Electrochim. Acta 52 (2007) 6561–6568.
11. C. Ocampo, C. Alemán, R. Oliver, M.L. Arnedillo, O. Ruiz, F. Estrany, *Polym. Int*. 56 (2007) 803–809.
12. J.R. Reynolds, J.P. Ruiz, A.D. Child, K. Nayak, D.S. Marynick, *Macromolecules* 24 (1991) 678–687.
13. K. R. J. Thomas, J. T. Lin, M. Velusamy, Y. T. Tao and C. H. Chuen, *Adv. Funct. Mater.*, 14, 83 (2004).
14. H.J. Yen, G.S. Liou, *Polym. Chem*. 3 (2012) 255–264.
15. H.J. Yen, H.Y. Lin, G.S. Liou, *Chem. Mater*. 23 (2011) 1874–1882.
16. K. Yamamoto, M. Higuchi, K. Uchida, Y. Kojima, *Macromolecules* 35 (2002) 5782–5788.
17. X.F. Cheng, J.S. Zhao, C.S. Cui, Y.Z. Fu, X.X. Zhang, *J. Electroanal. Chem.* 677–680 (2012) 24–30.
18. C.S. Cui, C.X. Xu, L.Y. Xu, J.S. Zhao, R.M. Liu, J. F. Liu, Q. P. He, H.S. Wang, *Opt. Mater,* 2011, 33(11), 1792-1799.
19. L.Y. Xu, J.S. Zhao, R.M. Liu, J.F. Liu, H.T. Liu, H.S. Wang, *Electrochim. Acta* 55 (2010) 8855-8862.
20. C. Zhang, Y. Xu, N. Wang, Y. Xu, W. Xiang, M. Ouyang, C. Ma, *Electrochim. Acta* 55 (2009) 13-18.
21. V. Seshadri, L.D. Wu, G.A. Sotzing, *Langmuir* 19 (2003) 9479-9485.
22. C. Kvarnstrom, H. Kulovaara, P. Damlin, T. Vuorinen, H. Lemmetyinen, A. Ivaska, *Synth. Met.* 149 (2005) 39.
23. G.M. Nie, L.Y. Qu, J.K. Xu, S.S. Zhang, *Electrochim. Acta* 53 (2008) 8351-8358.
24. S. Demoustier-Champagne, J. R. Reynolds, M. Pomerantz, *Chem. Mater.* 7 (1995) 277.
25. G. W. Lu, G. Q. Shi, *J. Electroanal. Chem.* 586 (2006) 154–160.
26. B. Yigitsoy, S. Varis, C. Tanyeli, I.M. Akhmedov, L. Toppare, *Electrochim. Acta*. 52 (2007) 6561–6568.
27. H.T. Liu, Y.Z. Li, J.K. Xu , Z.G. Le, M.B. Luo, B.S. Wang, S.Z. Pu, L. Shen, *Eur. Polym. J*., 44 (2008) 171-188.
28. D.M. de Leeuw, M.M.J. Simenon, A.R. Brown, R.E.F. Einerhand, *Synth. Met*. 87 (1997) 53–59.
29. J. Hwang, J.I. Son, Y.-B. Shim, *Sol. Energy Mater. Sol. Cells*. 94 (2010) 1286–1292.
30. Bin Wang, Jinsheng Zhao, Renmin Liu, Jifeng Liu, Qingpeng He, *Solar Energy Materials & Solar Cells.* 95 (2011) 1867–1874
31. M. Ouyang, G.H. Wang, C. Zhang, *Electrochim. Acta* 56 (2011) 4645–4649.

32. E. Yildiz, P. Camurlu, C. Tanyeli, I. Akhmedov, L. Toppare, *J. Electroanal. Chem*. 612 (2008) 247–256.
33. E. Sefer, F.B. Koyuncu, E. Oguzhan, S. Koyuncu, *J. Polym. Sci.: Part A: Polym. Chem*. 48 (2010) 4419–4427.
34. S. J. Yoo, J. H. Cho, J. W. Lim, S. H. Park, J. Jang, Y.-E. Sung, *Electrochem. Commun*. 12 (2010) 164–167.
35. G. A. Sotzing, J. R. Reynolds, *Chem. Mater*. 8 (1996) 882.
36. S. Koyuncu, B. Gultekin, C. Zafer, H. Bilgili, M. Can, S. Demic, İ. Kaya, S. Icli, *Electrochim. Acta.* 54 (2009) 5694-5702.
37. W.A. Gazotti, J.R.G. Casalbore-Micelli, A. Geri, M.A. De-Paoli, Adv. Mater. 10 (1998) 60.
38. C. Bechinger, M. S. Burdis, J. G. Zhang, *Solid State Commun*. 101 (1997) 753-756.